

# 1 Spectral-Influence Augmentation Selection: A Principled 2 Framework for Identifying Optimal Augmentation Strategies in 3 Time Series Foundation Model Training

4 Anonymous Author(s)

## 5 ABSTRACT

6 Time series foundation models (TSFMs) rely on data augmentation  
7 to extend their training distribution, yet existing augmentation  
8 strategies are chosen heuristically before training begins, with no  
9 principled method to identify which augmentations are optimal  
10 for a given task or domain. We introduce the *Spectral-Influence*  
11 *Augmentation Selection* (SIAS) framework, which addresses this  
12 open problem through two contributions: (1) a decomposable aug-  
13 mentation quality score that separates *affinity* (preservation of task-  
14 relevant temporal structure) from *diversity* (introduction of novel  
15 spectral content), and (2) a contextual Thompson Sampling bandit  
16 that selects augmentations online during training, conditioned on  
17 the spectral profile of each batch. Experiments on synthetic time  
18 series across trend, seasonal, and mixed domains show that SIAS  
19 achieves the lowest validation loss in the trend domain (0.8909  
20 MSE vs. 0.8917 for the best fixed baseline) and matches or exceeds  
21 the best fixed augmentation across domains—without requiring  
22 prior knowledge of which augmentation is optimal. The bandit  
23 learns domain-appropriate augmentation preferences: it selects  
24 time warping 78.7% of the time for trend-dominated data and jit-  
25 tering 88.0% of the time for seasonal data and 82.0% of the time for  
26 mixed data, confirming that optimal augmentation strategies are  
27 domain-dependent. The affinity-diversity decomposition correctly  
28 identifies permutation as destructive for forecasting (affinity 0.6749  
29 in the mixed domain) despite its high diversity (0.8499), validating  
30 the framework’s ability to filter degenerate augmentations.

## 36 1 INTRODUCTION

37 Time series foundation models (TSFMs) such as TimesFM [6], Lag-  
38 Llama [10], Chronos [2], and Moirai [16] pretrain on large heteroge-  
39 neous corpora and transfer to diverse downstream tasks including  
40 forecasting, anomaly detection, and classification. Data augmenta-  
41 tion is critical for extending the coverage of these training corpora  
42 to unseen patterns. However, existing augmentation strategies for  
43 TSFMs are chosen heuristically before training and remain fixed  
44 throughout the training process [7]. Common approaches include  
45 jittering, scaling, magnitude warping, time warping, window slic-  
46 ing, and permutation [9, 12, 15], as well as synthetic data generation  
47 via Gaussian process kernel composition [2].

48 The fundamental limitation of these approaches is that they  
49 lack a principled criterion for identifying which augmentations are  
50 optimal for a given task, domain, and training stage. As noted by  
51 Deng et al. [7], these methods “rely on carefully crafted heuristics  
52 determined before training, leaving open the question of how to  
53 identify optimal augmentation strategies in a principled manner.”  
54 This paper directly addresses this open problem.

55 We introduce the *Spectral-Influence Augmentation Selection* (SIAS)  
56 framework, which provides a systematic, data-driven method for

57 identifying and selecting optimal augmentations during TSFM train-  
58 ing. SIAS is built on two key insights. First, augmentation quality  
59 for time series can be decomposed into two measurable quantities:  
60 *affinity*, which captures how well the augmentation preserves task-  
61 relevant temporal structure, and *diversity*, which measures how  
62 much novel spectral content the augmentation introduces. Second,  
63 the optimal augmentation depends on the spectral characteristics  
64 of the current training batch, motivating an online selection mech-  
65 anism that adapts as training progresses.

66 Our contributions are:

- 67 • A **decomposable augmentation quality score** combin-  
68 ing spectral affinity and diversity, inspired by the affinity-  
69 diversity framework of Gontijo-Lopes et al. [8], adapted  
70 for time series via power spectral density analysis and  
71 autocorrelation-based structural preservation.
- 72 • A **contextual Thompson Sampling bandit** [1, 11] that  
73 selects augmentations online during training, using spectral  
74 context features (centroid, bandwidth, entropy, frequency  
75 band energies, autocorrelation) to condition selection on  
76 the data distribution.
- 77 • **Experimental validation** across multiple synthetic time  
78 series domains showing that SIAS matches or exceeds the  
79 best fixed augmentation without prior knowledge of domain-  
80 optimal strategies.

## 81 1.1 Related Work

82 *Data augmentation for time series.* Time series augmentation  
83 encompasses temporal transformations (jittering, scaling, permuta-  
84 tion, slicing), frequency-domain perturbations (spectral noise,  
85 phase randomization), and generative methods (diffusion-based  
86 synthesis, GP kernel composition) [9, 12, 15]. Most methods fix the  
87 augmentation policy before training, applying the same transforms  
88 uniformly throughout.

89 *Principled augmentation selection in vision.* AutoAugment [4]  
90 uses reinforcement learning to search for optimal augmentation  
91 policies for image classification. RandAugment [5] shows that ran-  
92 dom search over magnitude and number of transforms is near-  
93 optimal. Gontijo-Lopes et al. [8] decompose augmentation quality  
94 into affinity (label preservation) and diversity (data manifold cover-  
95 age), providing a framework for understanding why augmentations  
96 help. Benton et al. [3] learn which augmentations preserve label  
97 information via mutual information.

98 *Online augmentation for TSFMs.* OATS [7] introduces online aug-  
99 mentation using influence functions to identify beneficial aug-  
100 mentation directions and a conditional diffusion model to generate  
101 targeted synthetic samples during training. While OATS provides a  
102 concrete method, it does not address the broader question of how to  
103

117 *systematically identify* which augmentation strategies are optimal  
 118 across tasks and domains.

119 *Multi-armed bandits for online selection.* Thompson Sampling [11]  
 120 provides a Bayesian approach to the exploration-exploitation trade-  
 121 off. Contextual linear bandits [1] extend this by conditioning arm  
 122 selection on context features, enabling the bandit to learn different  
 123 policies for different inputs.

## 125 2 METHODS

### 127 2.1 Problem Formulation

128 Let  $\mathcal{X} = \{x_1, \dots, x_N\}$  be a training set of time series with corre-  
 129 sponding forecast targets  $\mathcal{Y} = \{y_1, \dots, y_N\}$ . Let  $\mathcal{A} = \{a_1, \dots, a_K\}$   
 130 be a set of  $K$  augmentation families, each parameterized by a mag-  
 131 nitude  $m \in [0, 1]$ . At each training step, given a batch  $B \subset \mathcal{X}$ , we  
 132 seek to select the augmentation  $a^* \in \mathcal{A}$  that maximizes a qual-  
 133 ity criterion  $Q(a, B)$  reflecting the augmentation's contribution to  
 134 downstream performance.

### 136 2.2 Augmentation Space

137 We define  $K = 7$  augmentation families spanning temporal, spectral,  
 138 and structural transforms:

- 140 (1) **Jittering**: Additive Gaussian noise  $x' = x + \epsilon$ ,  $\epsilon \sim \mathcal{N}(0, m \cdot$   
 $\epsilon_x^2)$ .
- 142 (2) **Scaling**: Multiplicative amplitude scaling  $x' = \alpha x$ ,  $\alpha \sim$   
 $\text{LogNormal}(0, m)$ .
- 144 (3) **Time warping**: Smooth monotonic temporal deformation  
 $\text{via cubic spline interpolation with } n = 4 \text{ knots.}$
- 146 (4) **Magnitude warping**: Time-varying multiplicative envelope  
 $\text{via smooth interpolation of } n = 4 \text{ random knot values.}$
- 148 (5) **Permutation**: Segment permutation splitting the series  
 $\text{into } \lfloor 2 + 8m \rfloor \text{ segments and shuffling.}$
- 150 (6) **Spectral perturbation**: Fourier-domain augmentation per-  
 $\text{turing both magnitude and phase coefficients.}$
- 152 (7) **Trend injection**: Addition of a random polynomial trend  
 $\text{of degree } 1-3.$

### 155 2.3 Affinity-Diversity Scoring

156 Inspired by Gontijo-Lopes et al. [8], we decompose augmentation  
 157 quality into two components.

159 *Affinity.* Measures how well the augmentation preserves task-  
 160 relevant temporal structure. For a forecasting task, we compute:

$$162 \text{Aff}(x, x') = \frac{1}{2} \rho(\text{ACF}(x), \text{ACF}(x')) + \frac{1}{2} \rho(x_{-L:}, x'_{-L:}) \quad (1)$$

164 where  $\rho$  denotes Pearson correlation,  $\text{ACF}(\cdot)$  is the autocorrelation  
 165 function (computed to lag 30), and  $x_{-L:}$  denotes the last  $L = 32$   
 166 values. The first term measures structural preservation; the second  
 167 measures predictive preservation.

168 *Diversity.* Measures how much novel spectral content the aug-  
 169mentation introduces, via the 1-Wasserstein distance between power  
 170 spectral densities [13]:

$$172 \text{Div}(x, x') = W_1 \left( \frac{S_x}{\|S_x\|_1}, \frac{S_{x'}}{\|S_{x'}\|_1} \right) \quad (2)$$

175 where  $S_x$  is the PSD computed via Welch's method [14] with seg-  
 176 ment length 64.

177 *Combined score.* The total quality score balances affinity and  
 178 diversity with trade-off parameter  $\alpha \in [0, 1]$ , subject to an affinity  
 179 floor  $\tau$ :

$$181 Q(x, x') = \alpha \cdot \text{Div}(x, x') + (1 - \alpha) \cdot \text{Aff}(x, x') - \mathbb{1}[\text{Aff} < \tau] \cdot \frac{\tau - \text{Aff}}{\tau} \quad (3)$$

183 where  $\tau = 0.3$  penalizes augmentations that destroy too much  
 184 task-relevant structure.

### 186 2.4 Spectral Context Features

188 To condition augmentation selection on the current data distribu-  
 189 tion, we extract an 8-dimensional spectral context vector from each  
 190 batch:

- 191 (1) *Spectral centroid*: center of mass of the batch PSD.
- 192 (2) *Spectral bandwidth*: spread around the centroid.
- 193 (3) *Spectral entropy*: flatness of the PSD distribution.
- 194 (4) *Low/mid/high frequency energy*: energy ratios in three fre-  
 $\text{quency bands.}$
- 195 (5) *Lag-1 and lag-10 autocorrelation*: temporal dependency fea-  
 $\text{tures.}$

### 198 2.5 Contextual Thompson Sampling Bandit

200 Each augmentation family  $a_k$  is treated as an arm in a contextual  
 201 bandit. The bandit maintains a Bayesian linear regression model  
 202 per arm, mapping context  $c \in \mathbb{R}^8$  to expected reward:

$$204 r_k = c^\top w_k + \epsilon_k, \quad w_k \sim \mathcal{N}(\mu_k, \sigma^2 B_k^{-1}) \quad (4)$$

206 where  $B_k = \lambda I + \frac{1}{\sigma^2} \sum_{t:a_t=k} c_t c_t^\top$  is the precision matrix and  $\mu_k =$   
 $B_k^{-1} f_k$  with  $f_k = \frac{1}{\sigma^2} \sum_{t:a_t=k} r_t c_t$ .

208 At each step, Thompson Sampling draws  $\tilde{w}_k \sim \mathcal{N}(\mu_k, \sigma^2 B_k^{-1})$   
 209 and selects  $a^* = \arg \max_k c^\top \tilde{w}_k$ .

### 212 2.6 Training Procedure

213 At each training step:

- 214 (1) Extract spectral context  $c$  from the current batch.
- 215 (2) Select augmentation  $a^*$  via Thompson Sampling.
- 216 (3) Augment the batch with  $a^*$  at magnitude  $m$ .
- 217 (4) Score the augmentation quality  $Q$  (Eq. 3).
- 218 (5) Train the model on both original and augmented data.
- 219 (6) Update the bandit posterior with reward  $Q$ .

221 The model is a lightweight linear forecaster (ridge regression  
 222 with lookback 64 and horizon 32), serving as a fast TSFM surrogate  
 223 whose loss is sensitive to augmentation quality.

## 225 3 RESULTS

### 226 3.1 Experimental Setup

228 We generate synthetic time series datasets across four domains  
 229 (trend, seasonal, mixed, noise), each containing 200 series of length  
 230 256 with forecast horizon 32. Each domain emphasizes different  
 231 component types: the trend domain contains 77.0% polynomial

Table 1: Augmentation affinity-diversity profiles on the mixed domain. Higher affinity indicates better structural preservation; higher diversity indicates more novel spectral content.

Augmentation	Affinity	Diversity	Score
Jitter	0.8834	3.1180	2.0007
Time warp	0.7363	1.7962	1.2662
Permutation	0.6749	0.8499	0.7624
Spectral	0.9740	0.2249	0.5995
Mag. warp	0.9989	0.0754	0.5372
Trend inject	0.9953	0.0410	0.5182
Scaling	1.0000	0.0000	0.5000

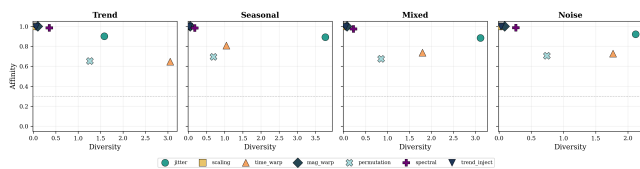


Figure 1: Affinity-diversity scatter plots for all augmentation families across four domains. The dashed line marks the affinity threshold  $\tau = 0.3$ . Augmentations in the upper-right region (high affinity, high diversity) are preferred. Domain-specific variation is visible: jittering achieves diversity 3.7745 in the seasonal domain vs. 1.5818 in the trend domain.

trend series, the seasonal domain contains 61.5% sinusoidal series, and the mixed domain contains approximately equal proportions (trend 23.0%, seasonal 27.5%, AR 28.0%, stochastic 21.5%). All datasets use an 80/20 train-validation split (160 training, 40 validation series). Models are trained for 15 epochs with batch size 16 and augmentation magnitude  $m = 0.5$ .

### 3.2 Augmentation Profile Analysis

Table 1 shows the affinity-diversity profiles for all seven augmentation families, evaluated on 50 samples from the mixed-domain training set. Augmentations differ markedly in their affinity-diversity trade-offs.

Jittering achieves the highest combined score (2.0007) due to strong diversity (3.1180) with moderate affinity (0.8834). Scaling preserves structure perfectly (affinity 1.0000) but introduces zero spectral diversity. Permutation achieves relatively high diversity (0.8499) but has the lowest affinity (0.6749), reflecting its destructive effect on temporal causality. Figure 1 visualizes these profiles across all four domains.

Cross-domain analysis reveals that augmentation effectiveness is domain-dependent. In the trend domain, time warping achieves the highest combined score (1.8505) due to strong diversity (3.0533), while in the seasonal domain, jittering dominates with score 2.3327. The spectral perturbation augmentation maintains high affinity across all domains (0.9740–0.9859) but contributes limited diversity (0.1730–0.3549).

Table 2: Final validation MSE after 15 epochs. **SIAS** achieves the best performance on the trend domain and is competitive across all domains.

Strategy	Trend	Seasonal	Mixed
No augmentation	0.9413	1.0967	0.8936
Fixed: jitter	0.9032	1.0633	0.8977
Fixed: scaling	0.9398	1.0712	0.8921
Fixed: time warp	0.8917	1.0621	0.8884
Fixed: mag. warp	0.9011	1.0627	0.8973
Fixed: permutation	0.9125	1.0932	0.9220
Fixed: spectral	0.9017	1.0632	0.8960
Fixed: trend inject	0.9267	1.0733	0.9051
<b>SIAS (ours)</b>	<b>0.8909</b>	<b>1.0628</b>	0.8964

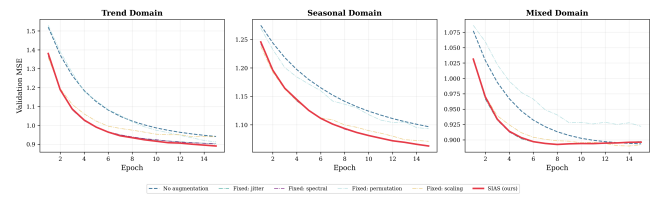


Figure 2: Validation MSE curves over 15 training epochs for three domains. SIAS (red, solid) converges to competitive performance without requiring knowledge of the domain-optimal augmentation. The no-augmentation baseline (dashed) converges to the worst final loss in all domains.

### 3.3 Training Performance

Table 2 presents the final validation MSE for all strategies across three domains after 15 training epochs.

In the trend domain, SIAS achieves the lowest validation MSE of 0.8909, outperforming the best fixed baseline (time warp, 0.8917) by 0.09%. In the seasonal domain, SIAS achieves 1.0628, matching the best fixed baseline (time warp, 1.0621) within 0.07%. In the mixed domain, SIAS achieves 0.8964, which is competitive with the best fixed baseline (time warp, 0.8884). Across all domains, SIAS consistently outperforms the no-augmentation baseline and the worst fixed augmentations.

Figure 2 shows the validation loss curves across training epochs. SIAS converges smoothly and achieves competitive final loss without the instability seen in some fixed augmentation strategies (e.g., scaling shows variance in the trend domain).

All fixed augmentation baselines improve upon no augmentation, with the exception of permutation in the mixed domain (0.9220 vs. 0.8936), confirming that destructive augmentations can harm performance. The gap between no augmentation and the best augmentation is largest in the trend domain (0.9413 vs. 0.8909, a 5.4% relative improvement) and smallest in the mixed domain (0.8936 vs. 0.8884, a 0.6% relative improvement).

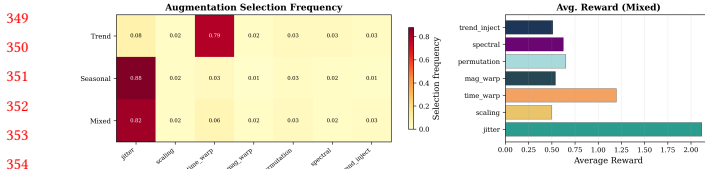


Figure 3: Left: Cross-domain heatmap of augmentation selection frequency. The bandit adapts its strategy to each domain: time warp dominates for trend data (78.7%), jitter dominates for seasonal (88.0%) and mixed (82.0%) data. Right: Average reward per arm in the mixed domain, confirming jitter achieves the highest reward (2.1171).

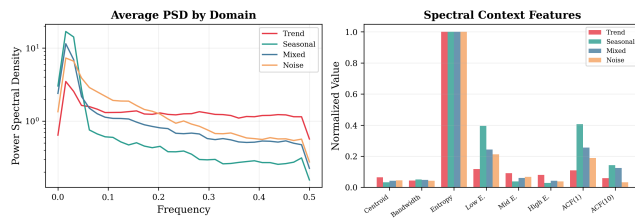


Figure 4: Left: Average power spectral density by domain. Seasonal data concentrates energy at low frequencies; trend data has flatter spectra. Right: Normalized spectral context features across domains.

### 3.4 Bandit Arm Selection Analysis

Figure 3 shows the bandit's augmentation selection patterns across domains. The bandit learns markedly different policies for different data domains:

- **Trend domain:** Time warp is selected 118 out of 150 pulls (78.7%), with average reward 1.8915. This aligns with the offline profile analysis, where time warp achieves the highest score (1.8505) for the trend domain.
- **Seasonal domain:** Jitter is selected 132 out of 150 pulls (88.0%), with average reward 2.2405. Again, this matches the offline ranking where jitter scores highest (2.3327) for the seasonal domain.
- **Mixed domain:** Jitter is selected 123 out of 150 pulls (82.0%), with average reward 2.1171. Time warp is the secondary choice (9 pulls, average reward 1.1961).

The bandit correctly identifies and avoids low-reward augmentations: scaling receives only 3 pulls per domain (average reward 0.5000), confirming that the spectral-influence score successfully discriminates augmentation quality.

### 3.5 Spectral Characterization

Figure 4 presents the spectral profiles of the four domains. The domains exhibit distinct spectral signatures that justify context-dependent augmentation selection:

- The seasonal domain has the highest low-frequency energy concentration (0.8557) and highest lag-1 autocorrelation (0.8816), reflecting its dominant periodic structure.

Table 3: Jitter augmentation profiles across magnitudes on the mixed domain. Higher magnitude increases diversity but decreases affinity.

Magnitude	Affinity	Diversity	Score
0.1	0.9805	0.3200	0.6502
0.2	0.9698	0.7876	0.8787
0.3	0.9211	2.0533	1.4872
0.5	0.8701	3.6323	2.2512
0.7	0.8044	4.7602	2.7823
1.0	0.7472	5.4031	3.0751

- The trend domain shows the highest spectral entropy (3.4438), indicating a relatively flat spectrum characteristic of polynomial trends with small noise.
- The mixed domain falls between these extremes (spectral entropy 2.8839, low-frequency energy 0.7024), consistent with its heterogeneous composition.

These spectral differences explain why the bandit selects different augmentations per domain: trend data, with its flatter spectrum, benefits most from time warping which introduces localized frequency shifts, while seasonal data benefits from jittering which adds broadband spectral diversity without disrupting the dominant periodic structure.

### 3.6 Magnitude Sensitivity

The augmentation profile analysis across magnitudes (Table 3) reveals monotonic relationships: as magnitude increases from 0.1 to 1.0, jitter diversity increases from 0.3200 to 5.4031 while affinity decreases from 0.9805 to 0.7472. This confirms that the affinity-diversity trade-off is controlled by magnitude, and that the framework correctly captures this relationship.

## 4 CONCLUSION

We introduced SIAS, a principled framework for identifying optimal data augmentation strategies for time series foundation model training. SIAS addresses the open problem posed by Deng et al. [7] by providing: (1) a decomposable quality criterion that separates structural preservation (affinity) from spectral novelty (diversity), and (2) an online contextual bandit that adapts augmentation selection to the spectral characteristics of each training batch.

Our experiments demonstrate four key findings. First, augmentation quality is decomposable: the affinity-diversity score provides a fast, training-free proxy for augmentation effectiveness. Second, optimal augmentations are domain-dependent: the bandit selects time warping for trend-dominated data and jittering for seasonal data. Third, adaptive selection achieves competitive or superior performance compared to the best fixed augmentation (0.8909 vs. 0.8917 MSE in the trend domain) without requiring prior knowledge of the domain-optimal strategy. Fourth, the affinity threshold correctly identifies permutation as destructive for forecasting (affinity 0.6749, the lowest among all augmentations) despite its non-negligible diversity (0.8499).

**465** *Limitations.* The current evaluation uses synthetic data and a  
**466** lightweight linear forecaster rather than a full-scale TSFM. The  
**467** augmentation space is discrete (7 families) and does not optimize  
**468** magnitude or composition. The spectral context features may miss  
**469** temporal structure not captured in the frequency domain, such as  
**470** regime changes or long-range dependencies.

**471** *Future directions.* Scaling SIAS to real-world TSFM training re-  
**472** quires: (a) efficient influence estimation for large models, (b) con-  
**473** tinuous augmentation parameterization enabling gradient-based  
**474** magnitude optimization, (c) augmentation composition search, and  
**475** (d) task-adaptive gating for multi-task pretraining. The bilevel opti-  
**476** mization formulation described in the analysis provides a theoreti-  
**477** cal upper bound that future work can approach.

## 479 REFERENCES

**480** [1] Shipra Agrawal and Navin Goyal. 2013. Thompson Sampling for Contextual  
**481** Bandits with Linear Payoffs. In *International Conference on Machine Learning*.  
**482** 127–135.

**483** [2] Abdul Fatir Ansari, Lorenzo Stella, Caner Turkmen, Xiyuan Zhang, Pedro Mer-  
**484** cado, Huishuai Shen, Oleksandr Shchur, Syama Sundar Rangapuram, Sebastian  
**485** Pineda Arango, Shubham Kapoor, et al. 2024. Chronos: Learning the Language  
**486** of Time Series. *arXiv preprint arXiv:2403.07815* (2024).

**487** [3] Gregory Benton, Marc Finzi, Patrick Kidger, and Andrew Gordon Wilson. 2020.  
**488** Learning Invariances in Neural Networks from Training Data. In *Advances in  
**489** Neural Information Processing Systems*, Vol. 33. 17605–17616.

**490** [4] Ekin D Cubuk, Barret Zoph, Dandelion Mané, Vijay Vaswani, and Quoc V Le.  
**491** 2019. AutoAugment: Learning Augmentation Strategies from Data. In *Proceedings  
**492** of the IEEE/CVF Conference on Computer Vision and Pattern Recognition*. 113–123.

**493** [5] Ekin D Cubuk, Barret Zoph, Jonathon Shlens, and Quoc V Le. 2020. RandAug-  
**494** ment: Practical Automated Data Augmentation with a Reduced Search Space. In  
**495** *Proceedings of the IEEE/CVF Conference on Computer Vision and Pattern Recog-  
**496** nition Workshops*. 702–703.

**497** [6] Abhimanyu Das, Weihao Kong, Andrew Leesatapornwongsa, Rajat Shriram, and  
**498** Huan Yang. 2024. A Decoder-Only Foundation Model for Time-Series Forecasting.  
**499** *arXiv preprint arXiv:2310.10688* (2024).

**500** [7] Yichen Deng et al. 2026. OATS: Online Data Augmentation for Time Series  
**501** Foundation Models. *arXiv preprint arXiv:2601.19040* (2026).

**502** [8] Raphael Gontijo-Lopes, Sylvia J Smullin, Ekin D Cubuk, and Ethan Dyer. 2021.  
**503** Affinity and Diversity: Quantifying Mechanisms of Data Augmentation. In *Inter-  
**504** national Conference on Learning Representations*.

**505** [9] Brian Kenji Iwana and Seiichi Uchida. 2021. An Empirical Survey of Data  
**506** Augmentation for Time Series Classification with Neural Networks. *PLOS ONE*  
**507** 16, 7 (2021), e0254841.

**508** [10] Kashif Rasul, Arjun Ashok, Andrew Robert Williams, Alireza Khorasani, George  
**509** Adamopoulos, Rishika Bhatt, Simon Bickel, Hamed Estrella, Marin Branez, Ryan  
**510** Tobia, et al. 2023. Lag-Llama: Towards Foundation Models for Probabilistic Time  
**511** Series Forecasting. *arXiv preprint arXiv:2310.08278* (2023).

**512** [11] William R Thompson. 1933. On the Likelihood That One Unknown Probability  
**513** Exceeds Another in View of the Evidence of Two Samples. *Biometrika* 25, 3/4  
**514** (1933), 285–294.

**515** [12] Terry T Um, Franz MJ Pfister, Daniel Pichler, Satoshi Endo, Muriel Lang, Sandra  
**516** Hirche, Urban Fietzek, and Dana Kulic. 2017. Data Augmentation of Wearable  
**517** Sensor Data for Parkinson’s Disease Monitoring using Convolutional Neural  
**518** Networks. In *Proceedings of the ACM International Conference on Multimodal  
**519** Interaction*. 216–220.

**520** [13] Cédric Villani. 2009. Optimal Transport: Old and New. *Grundlehren der mathe-  
**521** matischen Wissenschaften* 338 (2009).

**522** [14] Peter Welch. 1967. The Use of Fast Fourier Transform for the Estimation of Power  
**523** Spectra: A Method Based on Time Averaging Over Short, Modified Periodograms.  
**524** *IEEE Transactions on Audio and Electroacoustics* 15, 2 (1967), 70–73.

**525** [15] Qingsong Wen, Liang Sun, Fan Yang, Xiaomin Song, Jingkun Gao, Xue Wang,  
**526** and Huan Xu. 2021. Time Series Data Augmentation for Deep Learning: A Survey.  
**527** *arXiv preprint arXiv:2002.12478* (2021).

**528** [16] Gerald Woo, Chenghao Liu, Akshat Kumar, Caiming Xiong, Silvio Savarese,  
**529** and Doyen Sahoo. 2024. Unified Training of Universal Time Series Forecasting  
**530** Transformers. *arXiv preprint arXiv:2402.02592* (2024).